Anionic redox chemistry in Na-rich Na2Ru1–ySnyO3 positive electrode material for Na-ion batteries

Patrick Rozier, Mariyappan Sathiya, Alagar-Raj Paulraj, Dominique Foix, Thomas Desaunay, Pierre-Louis Taberna, Patrice Simon, Jean-marie Tarascon

Anionic redox chemistry in Na-rich $Na_2Ru_{1-y}Sn_yO_3$ positive electrode material for Na-ion batteries

Patrick Rozier [a,d,*], Mariyappan Sathiya [b,d], Alagar-Raj Paulraj [a], Dominique Foix [c,d], Thomas Desaunay [a,d], Pierre-Louis Taberna [a,d], Patrice Simon [a,d], Jean-Marie Tarascon [b,d,**]

[a] University of Toulouse III Paul Sabatier, CIRIMAT CNRS UMR 5085, 118 route de Narbonne, 31062, Toulouse Cedex 09, France
[b] FRE 3677 "Chimie du Solide et Energie", Collège de France, 11 Place Marcelin Berthelot, 75231, Paris Cedex 05, France
[c] IPREM/ECP (UMR 5254), University of Pau, 2 av. Pierre Angot, 64053, Pau Cedex 9, France
[d] Réseau sur le Stockage Electrochimique de l'Energie (RS2E), FR CNRS 3459, France

A B S T R A C T

The synthesis and Na- electrochemical activity of Na-rich layered $Na_2Ru_{1-y}Sn_yO_3$ compounds is reported. Like their Li-analogue, $Na_2Ru_{1-y}Sn_yO_3$ shows capacities that exceed theoretical capacity calculated from the cationic redox species. The high capacity was found, by means of XPS analysis, to be associated to the accumulation of both cationic (Ru^{4+}/Ru^{5+}) and anionic (O^{2-}/O_2^{n-}) redox processes. The structural evolutions during cycling have been followed and found to be associated with the cation disordering and loss of crystallinity on cycling.

Keywords:
Na-ion batteries
Cathode materials
Na-rich phases
Anionic redox activity

1. Introduction

Na-ion batteries promise to be an inexpensive and sustainable alternative to their Li counterpart since Na is abundant and widely spread over the world. However, performances of Na-based materials are hindered by the relatively higher atomic weight of Na and its larger atomic radius which limits the variety of materials where sodium can be reversibly extracted and inserted. Most research efforts have been focused on layered Na_xMO_2 [1,2] or NASICON [3] type structure that mimic Li-ion batteries positive electrode materials. Recently alkali-rich materials Li_2MO_3 have shown promising properties [4–8] as their experimental capacities exceed the theoretical value calculated according to the oxidation of the metallic species [6,8]. This extra capacity is associated, as shown in the case of $Li_2Ru_{1-x}Sn_xO_3$, to the high voltage redox activity of the anionic species [8]. To our knowledge only the study of Na_2RuO_3 analogous Na-rich oxide is reported [9]. It presents a layered structure [10] and electrochemical properties similar to that of Li-based analogue, however with an extra capacity of only 7% of the theoretical capacity [9].

In this work, we studied the electrochemical behavior of $Na_2Ru_{1-y}Sn_yO_3$ solid solution and report a large extra capacity in contradiction to what was reported for Na_2RuO_3. The replacement of active Ru^{4+} ion by the non-electrochemically active Sn^{4+} helps in isolating the contribution of conventional Ru^{4+}/Ru^{5+} redox mechanism and preliminary results indicate that the extra capacity is also associated to the anionic (O^{2-}/O_2^{n-}) redox couple.

2. Experimental

Stoichiometric amounts of RuO_2, SnO_2 and 10% excess of Na_2CO_3 (99.9% Sigma Aldrich) were mixed for the syntheses of $Na_2Ru_{1-y}Sn_yO_3$ ($y = 0; 0.25; 0.5; 0.75; 1$) samples. The reactants, hand grinded, are placed in a platinum crucible and introduced into a quartz tube. The sample is heated at 900 °C for 10 h under a flow of Argon, cooled down to room temperature and stored in an Argon-filled glove box. X-rays diffraction (XRD) patterns were recorded using a Bruker D8 diffractometer ($\lambda_{CuK\alpha} = 1.5418$ Å). Electrochemical tests were performed versus metallic Na in Swagelok-type cells. The active material is mixed with 20 wt.% carbon black. As all obtained results are independent of the salt $NaClO_4$ or $NaPF_6$ we used, we report only those obtained with a 1M $NaClO_4$ solution in a mixture of ethylene carbonate, propylene carbonate and dimethyl carbonate (9:9:2 weight ratio). Electrochemical tests were conducted at 20 °C using a Mac-pile or a VMP system operating in galvanostatic mode in the 1.5–4.2 V voltage range and with a C/20 rate (C = exchange of one mole of electron per mole of active material

* Correspondence to: P. Rozier, CIRIMAT 118 Route de Narbonne 31062 Toulouse Cedex 09, France. Tel.: +33 05 61 55 78 72.
** Correspondence to: J.-M. Tarascon, Collège de France 11 Place Marcelin Berthelot 75231 Paris Cedex 05 France. Tel.: +33 01 44 27 12 11.
E-mail addresses: rozier@chimie.ups-tlse.fr (P. Rozier), jean-marie.tarascon@college-de-france.fr (J.-M. Tarascon).

http://dx.doi.org/10.1016/j.elecom.2015.02.001

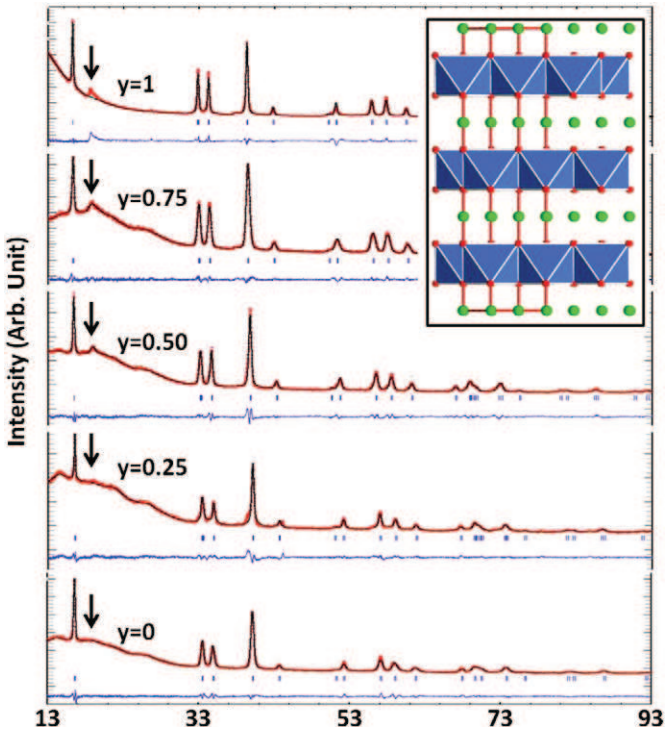

Fig. 1. XRD patterns for the $Na_2Ru_{1-y}Sn_yO_3$ solid solution. Inset shows a projection of the layered structure.

in 1 h). The in situ XRD study is conducted using a Swagelok-type cell equipped with a Beryllium window protected by an aluminum foil acting as current collector. The patterns are collected every 0.1 Na exchanged during electrochemical relaxation time and analyzed using the Rietveld method as implemented in the FullProf suite. XPS measurements were carried out using a Kratos Axis Ultra spectrometer. The data are collected using Al Kα radiation (1486.6 eV) and a 5.10^{-9} mbar pressure in the analysis chamber. The stability of the samples was analyzed using short acquisition time before normal collection condition with constant pass energy of 20 eV. The binding energy scale was calibrated using the *C1s* peak at 285.0 eV and the peak positions and areas were optimized by a weighted least-squares fitting method using 70% Gaussian, 30% Lorentzian line shapes. Quantification was performed on the basis of Scofield's relative sensitivity factors.

3. Results and discussion

Na_2RuO_3 [10] and Na_2SnO_3 [11] adopt the Na-rich layered structure corresponding to the stacking of alternating Na^+ and $[NaMO_3]^-$ layers (Fig. 1). The examination of the XRD patterns of the compounds (Fig. 1) shows that they can be indexed using the conventional hexagonal system. Extra peaks (close to $2\theta = 20°$) with intensity increasing with Sn content are indexed using monoclinic distortion of the cell. They show [12] that Sn is responsible for the ordering of the Na–Sn–Ru distribution in the layer. This relationship being beyond the scope of this study, for conciseness, the average description is kept. The cell parameters refinement, in agreement with the larger radius of Sn^{4+} (0.69 Å) than Ru^{4+} one (0.62 Å), indicate that the Sn^{4+} to Ru^{4+} substitution operates via a solid solution mechanism.

The electrochemical reactivity of $Na_2Ru_{1-y}Sn_yO_3$ series analyzed in Na-half cells shows that the first charge (Fig. 2a), despite similar with Li analogues, present a few differences. For the Sn free sample, there are three successive plateaus on charge which are less pronounced on the subsequent discharge (Fig. 2b) and progressively vanish upon long cycling. For the $y = 0.25$ sample, the three plateaus on charge exhibit a faster disappearance upon cycling (not observed during the second charge). For greater Sn concentration first charge exhibits only two plateaus which convert to S-like shape during discharge and subsequent cycles. This shows that a greater Sn content (>0.25) is needed for the Na-system, as compared to the Li-system (<0.25), to fully depart from the structural behavior of the parent A_2RuO_3 phases. The voltage of the two plateaus, respectively 2.8 V and 3.8 V vs Na^+/Na, is consistent with the voltage 3.6 V and 4.3 V vs Li^+/Li and the evolution of their capacity shows the same dependency with Ru content. During the first charge, the capacity of the low voltage plateau (2.8 V) corresponds to the removal of (1−y)Na in perfect agreement with oxidation of all the Ru^{4+} in $Na_2Ru_{1-y}Sn_yO_3$ samples. The capacity of the high voltage plateau (3.8 V) increases with the decrease of Ru and corresponds to 1.5 extracted Na for all the samples. During the first discharge, a loss in capacity is observed and increases with increasing Sn content thereby reducing the total reversible capacity. Then, all members of the $Na_2Ru_{1-y}Sn_yO_3$ solid solution exhibit capacity that largely exceeds the one calculated using only redox active Ru^{4+} ion, especially Na_2RuO_3 ($y = 0$) in contradiction with what was reported [9]. This apparent

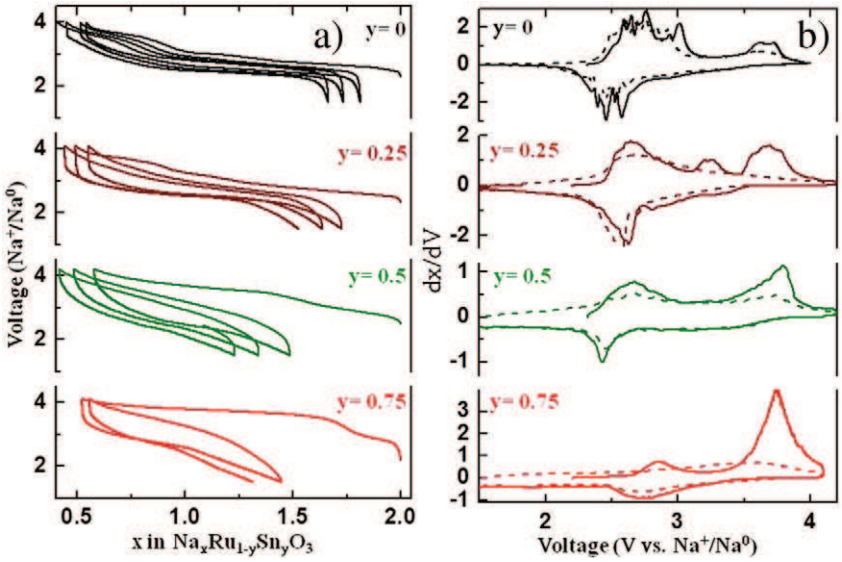

Fig. 2. $Na_2Ru_{1-y}Sn_yO_3$ electrochemical behavior a) voltage composition curve and b) derivative plots.

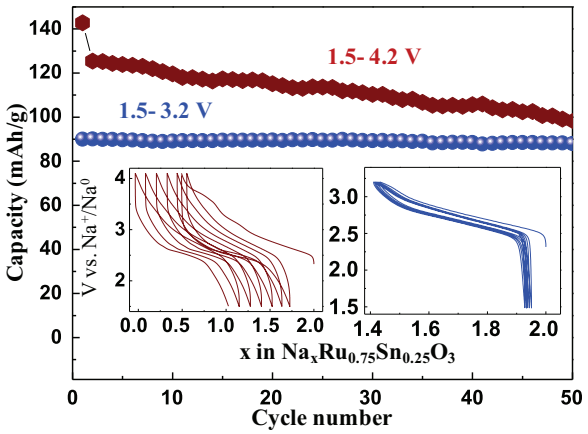

Fig. 3. Cycling behavior of the $Na_2Ru_{0.75}Sn_{0.25}O_3$ sample.

contradiction is explained by the high sensitivity to moisture and spontaneous oxidation of the Sn free Na_2RuO_3 sample which hampered the accurate investigation of the extra-capacity phenomenon as recently confirmed [13]. The increase of Sn content leads to an increase of the high voltage plateau capacity up to 1 and 1.3 Na^+ together with a larger Na lost between the first charge and discharge which reaches nearly 0.46 and 0.56 Na^+ for the y = 0.5 and 0.75 samples respectively. The investigation of the cycling behavior of $Na_2Ru_{0.75}Sn_{0.25}O_3$ shows (Fig. 3) that a voltage cut-off limited to the charging of Ru^{4+}/Ru^{5+} alone leads to ~100% capacity retention even after 50 cycles while increasing the charging voltage to 4.2 V reduces the capacity from 140 mAh/g to 100 mAh/g on cycling to 50 cycles. This confirms that the irreversible capacity is associated to the high voltage phenomenon which was already observed in some analogous Li-rich phases. Effectively, whatever the value of y in the $Li_2Ru_{1-y}Sn_yO_3$ system, the amplitude of the first and second plateau were nearly equal as expected according to the proposed dual cationic-redox anionic processes [8]. Deviation from the above relation (increase of the high voltage plateau correlated to an increase in the irreversibility), already observed with the $Li_2Ru_{1-y}Mn_yO_3$ systems, was assigned to the irreversible release of O_2 from the sample [7]. This implies that for the $Na_2Ru_{1-y}Sn_yO_3$ system, the y = 0.5 and y = 0.75 samples show the formation of oxygenated species prior to reach a potential domain over which the samples loose irreversibly O_2, hence rendering such compositions poorly attractive. For such a reason, $Na_2Ru_{0.75}Sn_{0.25}O_3$ sample is selected to further structural and XPS characterizations.

In situ XRD performed on $Na_xRu_{0.75}Sn_{0.25}O_3$ sample (Fig. 4a) shows that the charge starts via a solid solution mechanism indicating that the voltage-composition curve should be considered as a flat S-shaped curve instead of a real 2.8 V plateau as previously suggested. Cell parameters refinement shows that the removal of Na ions is associated with an increase of the interlayer space in agreement with an increase of repulsive effects between layers and a decrease of the layer length in agreement with the diminution of Ru ion radius during oxidation. This indicates that in the first part of the charge Na is removed from the interlayer space thus reducing the screening effect and that the Ru redox couple is active. Further charging below x = 1.3 is associated with the extraction of Na from the mixed $Na_{1/3}M_{2/3}$ layers and corresponds to the growth of a second phase at the expense of the pristine one which becomes a single phase for x = 1.0. Despite a poor quality of XRD pattern, all peaks can be assigned using the cell setting of pristine one. Cell parameters refinements indicate a brutal change between the pristine phase (a = 3.09 Å c = 16.52 Å) and the second phase (a = 3.04 Å c = 15.88 Å) which results in a decrease of the cell volume from 137 $Å^3$ to 127 $Å^3$. On subsequent discharge, this two steps process is reversible, as witnessed by the shift back of lattice parameters to those of the pristine phase. Nevertheless, the XRD profile show broader Bragg peaks with the absence of superstructure peaks indicating the onset of a Na-driven disorder through the first charge–discharge cycle.

This solid solution–biphasic–solid solution process is exactly the opposite of the one reported for Li analogues [8] (biphasic domain then solid solution operating on the second phase) confirming, as widely reported, the drastically different room temperature Li(Na)-driven phase diagrams associated, among others, to both the size and polarity differences between Li and Na ions.

XPS analyses have been carried out on pristine, charged to 2.8 V and 4.3 V, and charge–discharged to 1.5 V electrode materials and valence state evolution confirmed by EPR analysis as previously reported for Li based compounds. They indicate that Sn is not active and Ru^{4+} is oxidized up Ru^{+5} during the 2.8 V process (not shown). Characterization of the O1s band (Fig. 4c) confirms that O is not affected by the charge on the 2.8 V plateau while an extra band observed at higher bending energy is observed for the fully charged sample. These phenomena, fully reversible on discharge, and compared with Li based compound investigation [8], are in perfect agreement with the presence of

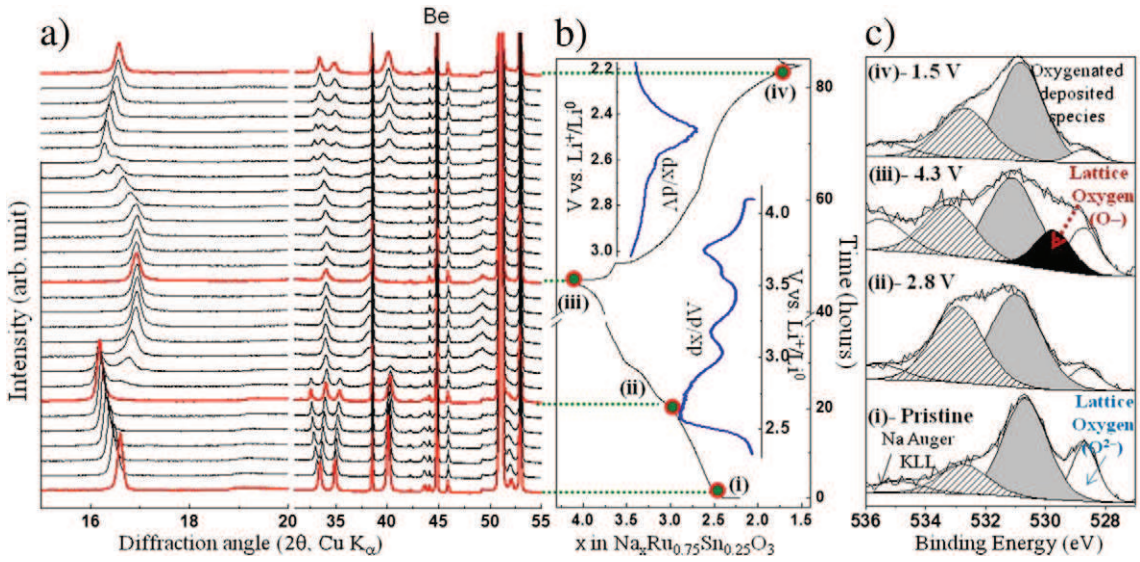

Fig. 4. Characterization of $Na_2Ru_{0.75}Sn_{0.25}O_3$ sample a) insitu XRD patterns; b) voltage profile; and c) O1s XPS spectra.

oxygenated $(O_2)^{n-}$ species and confirm that the redox activity of anion is effective and responsible for the extra capacity observed for these samples.

4. Conclusion

We have reported the structural–electrochemical study of Na-rich $Na_2Ru_{1-y}Sn_yO_3$ compounds and show that, like their Li analogues, they present large capacities resulting from both cationic ($Ru^{4+} \rightarrow Ru^{5+}$) and anionic ($O^{2-} \rightarrow O_2^{n-}$) redox processes as deduced from XPS spectroscopy. Therefore, in contrast to the Li series, such a formation of oxygen species is followed, for the Sn rich samples, by the irreversible loss of O_2. The differences in both the size and polarity of Na^+ as compared to Li^+, which lead to different Na-driven structural changes, are most likely at the origin of the increasing instability of the oxygenated species towards the release of O_2. Scanning transmission electron microscopy imaging methods and electron energy loss spectroscopy for simultaneous mapping of the oxidation state and coordination number of the transition metal cations, are presently being conducted to assess not only the local structure, but also the local chemistry of these Na electrodes. This work which shows for the first time the feasibility of the Na-rich layered phases to have high capacities due the anionic redox activity contribution opens the way to design new positive electrode materials for Na-ion batteries with the possibility to exchange at high voltage more than 1 electron per transition metal. It now remains to chemically manipulate these Na-rich based layered compounds to enhance their cycling behavior and stability against moisture so that they could be handled in air.

Conflict of interest

There is no conflict of interest.

References

[1] D. Kim, S.-H. Kang, M. Slater, S. Rood, J.T. Vaughey, N. Karan, M. Balasubramanian, C. Johnson, Enabling sodium batteries using lithium-substituted sodium layered transition metal oxide cathodes, Adv. Energy Mater. 1 (2011) 333–336.

[2] N. Yabuuchi, M. Kajiyama, J. Iwatate, H. Nishikawa, S. Hitomi, R. Okuyama, R. Isio, Y. Yamada, S. Komaba, P2-type Nax[$Fe_1/_2Mn_1/2$]O_2 made from earth-abundant elements for rechargeable Na batteries, Nat. Mater. 11 (2012) 512–517.

[3] K. Saravanan, C.W. Mason, A. Rudola, K.H. Wong, P. Balaya, First report on excellent cycling stability and superior rate capability of $Na_3V_2(PO_4)_3$ for sodium ion batteries, Adv. Energy Mater. 3 (2013) 444–450.

[4] Z. Lu, L.Y. Beaulieu, R.A. Donaberger, C.L. Thomas, J.R. Dahn, Synthesis, structure, and electrochemical behavior of Li [$Ni_xLi_{1/3-2x/3}Mn_{2/3-x/3}$]$O_2$, J. Electrochem. Soc. 149 (2002) A778.

[5] C.S. Johnson, J.-S. Kim, C. Lefief, N. Li, J.T. Vaughey, M.M. Thackeray, The significance of the Li_2MnO_3 component in 'composite' $xLi_2MnO_3 \cdot (1-x)LiMn_{0.5}Ni_{0.5}O_2$ electrodes, Electrochem. Commun. 6 (2004) 1085–1091.

[6] A.R. Armstrong, M. Holzapfel, P. Novak, C.S. Johnson, S.-H. Kang, M.M. Thackeray, P.G. Bruce, Demonstrating oxygen loss and associated structural reorganization in the lithium battery cathode Li[$Ni_{0.2}Li_{0.2}Mn_{0.6}$]O_2, J. Am. Chem. Soc. 128 (2006) 8694–8698.

[7] M. Sathiya, K. Ramesha, G. Rousse, D. Foix, D. Gonbeau, A.S. Prakash, M.-L. Doublet, K. Hemalatha, J.-M. Tarascon, High performance $Li_2Ru_{1-y}Mn_yO_3$ ($0.2 \leq y \leq 0.8$) cathode materials for rechargeable lithium-ion batteries: their understanding, Chem. Mater. 25 (2013) 1121–1131.

[8] M. Sathiya, G. Rousse, K. Ramesha, C.P. Laisa, H. Vezin, M.T. Sougrati, M.-L. Doublet, D. Foix, D. Gonbeau, W. Walker, A.S. Prakash, M. Ben Hassine, L. Dupont, J.-M. Tarascon, Reversible anionic redox chemistry in high-capacity layered-oxide electrodes, Nat. Mater. 12 (2013) 827–835.

[9] M. Tamaru, X. Wang, M. Okubo, A. Yamada, Layered Na_2RuO_3 as a cathode material for Na-ion batteries, Electrochem. Commun. 33 (2013) 23–26.

[10] K.M. Mogare, K. Friese, W. Klein, M. Jansen, Syntheses and crystal structures of two sodium ruthenates: Na_2RuO_4 and Na_2RuO_3, Z. Anorg. Allg. Chem. 630 (2004) 547–552.

[11] JCPDS card n 00-030-1252.

[12] L. Viciu, J.W.G. Bos, H.W. Zandbergen, Q. Huang, M.L. Foo, S. Ishiwata, A.P. Ramirez, M. Lee, N.P. Ong, R.J. Cava, Crystal structure and elementary properties of Na_xCoO_2 ($x = 0.32, 0.51, 0.6, 0.75$, and 0.92) in the three-layer $NaCoO_2$ family, Phys. Rev. B 73 (2006) 174104.

[13] M. Tamaru, X. Wang, M. Okubo, A. Yamada, Corrigendum to "Layered Na2RuO3 as a cathode material for Na-ion batteries" [Electrochemistry communications 33 (2013) 23–26], Electrochem. Commun. 34 (2013) 360.